

Scavenger receptor CD36 mediates uptake of high density lipoproteins in mice and by cultured cells^[S]

May Brundert,* Joerg Heeren,* Martin Merkel,* Antonella Carambia,* Johannes Herkel,* Peter Groitl,[†] Thomas Dobner,[†] Rajasekhar Ramakrishnan,[§] Kathryn J. Moore,** and Franz Rinninger^{1,*}

University Hospital Hamburg Eppendorf,* Hamburg, Germany; Heinrich Pette Institute for Virology,[†] 20246 Hamburg, Germany; Columbia University College of Physicians and Surgeons,[§] New York, NY 10032; and New York University Medical Center,** New York, NY 10016

Abstract The mechanisms of HDL-mediated cholesterol transport from peripheral tissues to the liver are incompletely defined. Here the function of scavenger receptor cluster of differentiation 36 (CD36) for HDL uptake by the liver was investigated. CD36 knockout (KO) mice, which were the model, have a 37% increase ($P = 0.008$) of plasma HDL cholesterol compared with wild-type (WT) littermates. To explore the mechanism of this increase, HDL metabolism was investigated with HDL radiolabeled in the apolipoprotein (¹²⁵I) and cholesteryl ester (CE, [³H]) moiety. Liver uptake of [³H] and ¹²⁵I from HDL decreased in CD36 KO mice and the difference, i. e. hepatic selective CE uptake ([³H]¹²⁵I), declined (−33%, $P = 0.0003$) in CD36 KO compared with WT mice. Hepatic HDL holo-particle uptake (¹²⁵I) decreased (−29%, $P = 0.0038$) in CD36 KO mice. In vitro, uptake of ¹²⁵I-/[³H]HDL by primary liver cells from WT or CD36 KO mice revealed a diminished HDL uptake in CD36-deficient hepatocytes. Adenovirus-mediated expression of CD36 in cells induced an increase in selective CE uptake from HDL and a stimulation of holo-particle internalization. **In conclusion, CD36 plays a role in HDL uptake in mice and by cultured cells. A physiologic function of CD36 in HDL metabolism in vivo is suggested.**—Brundert, M., J. Heeren, M. Merkel, A. Carambia, J. Herkel, P. Groitl, T. Dobner, R. Ramakrishnan, K. J. Moore, and F. Rinninger. Scavenger receptor CD36 mediates uptake of high density lipoproteins in mice and by cultured cells. *J. Lipid Res.* 2011. 52: 745–758.

Supplementary key words adrenal • cholesteryl ester • HDL • liver • selective

High density lipoprotein plays a critical role in cholesterol homeostasis (1). This lipoprotein fraction presumably removes cholesterol from peripheral tissues, such as the vessel

wall. After esterification in plasma, HDL-associated cholesteryl esters (CE) are delivered to other lipoprotein fractions or tissues (1, 2). One mechanism that mediates the direct delivery of HDL-associated CE to organs is the selective lipid uptake pathway (2). In this process, HDL CE is internalized by cells independently of the uptake of the HDL holo-particle. This selective lipid uptake appears to be important for the transport of cholesterol to steroidogenic tissues for hormone biosynthesis and to the liver. In the liver, HDL-derived cholesterol can be secreted into bile, used for bile acid synthesis, or packaged and secreted in newly synthesized lipoproteins.

Scavenger receptors mediate the cellular uptake of lipoproteins (3, 4). Scavenger receptor class B type I (SR-BI) and cluster of differentiation 36 (CD36) are members of class B of this family (3, 5). As plasma membrane-associated proteins, structurally both molecules comprise extracellular loops that are anchored in the membrane by transmembrane domains adjacent to short cytoplasmic tails. A high degree of sequence homology is detected throughout the extracellular loop domains between SR-BI and CD36; however, the cytoplasmic and the transmembrane domains have limited sequence similarity (4).

SR-BI is expressed abundantly in the liver and steroidogenic tissues (3). This receptor binds HDL with high affinity and mediates selective uptake of HDL CE in the liver and adrenals (6). In mice, hepatic SR-BI overexpression promotes selective HDL CE uptake by the liver (7). In contrast, mice

Abbreviations: CD36, cluster of differentiation 36; CE, cholesteryl ester; CEt, cholesteryl oleyl ether; CETP, cholesteryl ester transfer protein; FCR, fractional catabolic rate; FPLC, fast protein liquid chromatography; KC, Kupffer cell; KO, knockout; LRP1, low density lipoprotein receptor-related protein1; LSEC, liver sinusoidal endothelial cells; MOI, multiplicity of infection; SR-BI, scavenger receptor class B type I; TC, tyramine cellobiose; WT, wildtype.

¹To whom correspondence should be addressed.

e-mail Rinninger@uke.uni-hamburg.de

^[S]The online version of this article (available at <http://www.jlr.org>) contains supplementary data in the form of one figure and one table.

This work was supported by Grant Ri 436/8-1 from Deutsche Forschungsgemeinschaft (DFG), Bonn, Germany, and by Werner Otto Stiftung, Hamburg, Germany.

Manuscript received 11 October 2010 and in revised form 23 December 2010.

Published, JLR Papers in Press, January 8, 2011

DOI 10.1194/jlr.M011981

Copyright © 2011 by the American Society for Biochemistry and Molecular Biology, Inc.

This article is available online at <http://www.jlr.org>

with a targeted mutation in the SR-BI gene have a decrease in selective CE uptake (6, 8, 9). Thus SR-BI is a physiologically relevant HDL receptor with a function in cholesterol homeostasis in vivo.

The role of CD36 in lipoprotein metabolism is less well defined (4). This molecule is expressed in skeletal and heart muscle, liver, lungs, adipose tissue, spleen, small intestine, testis, capillary endothelium, microglia, and elicited peritoneal macrophages (10, 11). The ligands of CD36 include native and oxidized lipoproteins, anionic phospholipids, thrombospondin, collagen, amyloid β , and plasmodium falciparum-infected erythrocytes (4, 5, 11, 12). With respect to metabolism, CD36 facilitates the transfer of fatty acids into myocytes (10). Recently a role of CD36 for selective CE uptake from low density lipoprotein was proposed (11). On the basis of this broad ligand specificity and its widespread expression, diverse functions of CD36 have been suggested, including atherogenesis and lipoprotein metabolism (4).

In vitro, the function of scavenger receptor CD36 in HDL metabolism was compared with the respective role of SR-BI (12–14). CD36 and SR-BI bind HDL with high affinity, and both receptors mediate selective HDL CE uptake. However, the rate of selective uptake mediated by CD36 is lower compared with the uptake mediated by SR-BI. These studies were performed in cell lines overexpressing CD36, and therefore, the relevance of these in vitro experiments for the role of CD36 in HDL metabolism in vivo was not established.

In CD36-deficient mice, the function of CD36 for HDL metabolism was explored (15, 16). Mice with a targeted mutation in the CD36 gene have a significant increase in plasma HDL cholesterol compared with wildtype (WT) littermates. Therefore, a role of CD36 in HDL metabolism in vivo was suggested (15, 16). With respect to the mechanism of this increase in HDL, a recent study proposed that a deficiency of CD36 may promote HDL formation. A lack of CD36 may be associated with increased hepatic cholesterol and phospholipid efflux and a stimulated hepatic secretion of apolipoproteins. These changes may represent a mechanism that mediates an increase in plasma HDL cholesterol. However, in these studies, the role of CD36 for HDL catabolism in mice was not exhaustively addressed (16).

In this study, the role of CD36 for HDL catabolism was investigated in mice. Metabolic experiments were performed using murine HDL which was radiolabeled in the apolipoprotein (^{125}I) as well as in the lipid (CE, [^3H]) moiety (2). In CD36-deficient mutant mice, experiments with ^{125}I -/ ^3H]HDL showed diminished selective HDL CE uptake and reduced HDL holo-particle internalization by liver and adrenal glands compared with WT littermates. In cultured hepatocytes from CD36-deficient liver, selective CE uptake and HDL holo-particle internalization from ^{125}I -/ ^3H]HDL declined. In contrast, adenovirus-mediated overexpression of CD36 in cultured cells stimulated cellular HDL uptake. In summary, evidence is presented that CD36 mediates HDL uptake by tissues and thus plays a physiologic role in the catabolism of this atheroprotective lipoprotein fraction in vivo.

Materials

Primers were purchased from Metabion. Taq-DNA polymerase, a fluorometric cholesterol assay, culture media, sera, and supplements for cell culture were supplied by Invitrogen. The 6-well tissue culture plates were obtained from Becton Dickinson. Collagenases were from Worthington (hepatocytes) or from Serva (non-parenchymal liver cells). ^{125}I iodine, [^3H]cholesteryl oleyl ether, [^{14}C]oleate, and ECL reagent were purchased from GE Healthcare. Heparin, protease inhibitor cocktail “complete,” and enzymatic assays for cholesterol, HDL cholesterol, and triglyceride were supplied by Roche. Assays for phospholipid, unesterified cholesterol, and fatty acids were obtained from Wako. BSA, iodoxanol gradient medium, and standard laboratory chemicals were purchased from Sigma Aldrich. Horseradish peroxidase-conjugated secondary antibodies were supplied by Dianova. Scintillation cocktail was from PerkinElmer. Nitrocellulose membrane was obtained from Schleicher and Schuell. Films were supplied by Kodak. Rodent chow was purchased from Sniff.

Mice

Male mice with a targeted mutation in the CD36 gene [CD36 $^{-/-}$, knockout (KO), homozygous] and the respective male littermate controls (WT) were used in this study (17). All animals were on a C57BL/6J genetic background. The genotype of each mouse was analyzed by PCR from genomic DNA isolated from tail biopsies (17). Mice were maintained on a standard laboratory chow diet and had unlimited access to food and water. The age of the rodents used in this study was between 20 and 50 weeks. All animal protocols were approved by the Institutional Animal Care and Use Committee of the University Hospital Hamburg.

Lipoprotein preparation

Mice were fasted for 4 h before blood harvest. HDL ($d = 1.063\text{--}1.21\text{ g/ml}$) was isolated from WT murine plasma by sequential ultracentrifugation (18).

Murine HDL was doubly labeled with ^{125}I -tyramine cellobiose (^{125}I -TC) in the apolipoprotein and with [^3H]cholesteryl oleyl ether ([^3H]CET) in the CE moiety (9, 19). [^3H]CET was introduced in ^{125}I -TC-HDL by exchange from donor liposomal particles, which contained [^3H]CET, using partially purified human plasma cholesteryl ester transfer protein (CETP) (20). The final ^{125}I -TC-/ ^3H]CET-HDL preparation was extensively dialyzed against PBS (pH 7.4) containing EDTA (1 mmol/l). Both HDL tracers were intracellularly trapped after uptake by tissues and cells and were not released thereafter (19).

HDL metabolism in mice

For plasma decay analysis of ^{125}I -TC-/ ^3H]CET-HDL, the mice were fasted for 4 h before tracer injection (2). Then ^{125}I -TC-/ ^3H]CET-HDL (30 μg HDL protein per mouse) was injected in a tail vein. Thereafter, blood samples (30 μl per time point) were collected periodically (10 and 30 min; 2, 5, 9, 22, and 24 h) after injection. Animals were fasted throughout the 24 h study period but had unlimited access to water. Plasma aliquots were directly assayed for ^{125}I radioactivity, and [^3H] was analyzed after lipid extraction (21). Computer modeling was used to fit (by method of least squares) multiexponential curves arising from a common two-pool model simultaneously to both tracers' plasma decay data and to calculate plasma fractional catabolic rates (plasma FCRs) for the two tracers (22). The modeling was done separately for the data from each mouse, so that individual plasma FCRs for both tracers were calculated for each animal.

Tissue sites of uptake of HDL-associated tracers were determined 24 h after injection of ^{125}I -TC-/ ^3H]CEt-HDL, when both tracers were predominantly cleared from plasma (2). Finally the animals were anesthetized, the abdomen and chest were opened, and a catheter was inserted into the heart. The inferior vena cava was cut and the mice were perfused extensively with saline (50 ml per animal). After perfusion, the liver, adrenals, kidneys, brain, heart, lungs, spleen, stomach, intestine, and carcass of each mouse were harvested and homogenized. Homogenates from each tissue and the carcass were directly assayed for ^{125}I radioactivity, and aliquots were analyzed for ^3H after lipid extraction (21).

Total radioactivity recovered from all tissues and the carcass of each mouse was calculated (2). The fraction of total tracer uptake attributed to a specific organ was calculated as the radioactivity recovered in that organ divided by the total radioactivity recovered from all tissues and carcass. Thus the percentage of recovered extravascular radioactivity in tissues was determined 24 h after injection of labeled HDL.

To allow comparison of the specific activities of various tissues in HDL internalization and to directly compare the rates of uptake of the apolipoprotein component and the CE moiety of HDL, the data were expressed as organ fractional catabolic rates (organ FCR) (2). These rates were calculated as follows: (Organ FCR in Tissue X) = (Plasma FCR) \times (Fraction [%] of Total Body Tracer Recovery in Tissue X). This organ FCR represents the fraction of the plasma pool of either HDL tracer cleared by an organ per h. ^{125}I -TC represents the uptake of HDL holo-particles by tissues (19). Selective HDL CE uptake is calculated as the difference in organ FCR between ^3H]CEt and ^{125}I -TC.

Preparation of hepatocytes

Primary hepatocytes were isolated from murine liver by perfusion (37°C, 18 minutes) with Hanks balanced salt solution supplemented with collagenase (0.3 mg/ml, type I), Hepes (10 mMol/l), and protease inhibitor mixture "complete" (23). The cells then were cultured (37°C, 2.0 h) in DMEM containing FBS (5%, v/v), penicillin (100 $\mu\text{g}/\text{ml}$), and streptomycin (100 $\mu\text{g}/\text{ml}$). Finally the culture medium was aspirated, and the cells were washed three times in PBS. Hepatocytes were used for ^{125}I -TC-/ ^3H]CEt-HDL uptake assays or for preparation of postnuclear supernatants (24, 25).

Preparation of nonparenchymal liver cells

Non-parenchymal hepatic cells were prepared from murine liver as described (26). Briefly, the liver was perfused (37°C) through the portal vein with calcium-free phosphate buffer supplemented with collagenase (0.05%, w/v, type A). Then the organ was mechanically disrupted and incubated (37°C, 30 minutes) in Gray's balanced saline containing collagenase (0.05%, w/v, type IV) with constant rotation (240 rpm). The cell suspension was passed through a cell sieve to remove debris. Nonparenchymal liver cells were recovered by centrifugation using an iodixanol density gradient (30%). Finally, cells were cultured (37°C, 2.0 h) in DMEM containing FBS (5%, v/v), penicillin (100 $\mu\text{g}/\text{ml}$), and streptomycin (100 $\mu\text{g}/\text{ml}$). The culture medium was aspirated, and the cells were washed three times in PBS. These cells were used for ^{125}I -TC-/ ^3H]CEt-HDL uptake assays (25). Nonparenchymal liver cells were predominantly composed of Kupffer cells (KC) and liver sinusoidal endothelial cells (LSEC). No hepatocytes were detected in this preparation (26).

Generation of recombinant adenoviral vectors and infection of H1299 cells

The recombinant, replication-defective adenoviruses Ad-mCD36 and Ad-GFP were generated as outlined (27). Briefly, Ad-mCD36 contains an expression cassette encoding the murine

CD36 cDNA; the sequence was inserted into vector AdEasy. Ad-GFP (control) contains no transgene expression cassette.

H1299 cells were incubated (37°C) in DMEM supplemented with FBS (10%, v/v), penicillin (100 $\mu\text{g}/\text{ml}$), and streptomycin (100 $\mu\text{g}/\text{ml}$) (28). At 24 h after plating H1299 cells in wells (35 mm), no virus (mock, DMEM), Ad-GFP, or Ad-mCD36 were added. H1299 cells were exposed for 72 h to a multiplicity of infection (MOI) of 200 virus particles per cell.

Uptake assay for radiolabeled HDL

Hepatocytes, nonparenchymal liver cells, or H1299 cells were incubated (37°C, 2.0 or 4.0 h) in DMEM containing BSA (5 mg/ml), penicillin (100 $\mu\text{g}/\text{ml}$), streptomycin (100 $\mu\text{g}/\text{ml}$), and the respective ^{125}I -TC-/ ^3H]CEt-HDL (25). Finally cells were harvested by trypsin/EDTA (1 \times , trypsin 0.05%, EDTA 0.53 mmol/l) treatment and cellular uptake of HDL tracers was measured. ^{125}I was directly radioassayed and ^3H was analyzed after lipid extraction (21). Uptake of ^{125}I -TC-/ ^3H]CEt-HDL by cells was shown in terms of apparent HDL particle uptake, expressed as HDL protein (2, 25), to compare the uptake of both tracers on a common basis. The uptake of HDL holo-particles is represented by ^{125}I -TC, and the difference between ^3H]CEt and ^{125}I -TC yields apparent selective HDL CE uptake by cells (19).

Immunoblots

Membrane fractions (29) from murine liver or adrenals and postnuclear supernatants (24) from cultured primary hepatocytes and H1299 cells were prepared. Protease inhibitor cocktail "complete" was present during these preparations.

Membrane fractions or postnuclear supernatants were boiled (93°C, 10 minutes) and separated by SDS polyacrylamide gel (10%) electrophoresis under reducing conditions (mercaptoethanol) and then transferred to a nitrocellulose membrane (9). The blots were probed with anti-CD36 (rabbit polyclonal antiserum against murine CD36) (30), anti-SR-BI (rabbit polyclonal antibody to murine SR-BI, Novus Biologicals), anti-LRP1 (sheep anti-LRP1 antibody, raised against a synthetic peptide from human LRP1) (31), or anti- β -Actin (monoclonal anti- β -Actin, mouse, Sigma Aldrich) as primary antibodies. β -Actin was used as loading control. Finally the blots were incubated with appropriate horseradish peroxidase-conjugated secondary antibodies and developed with ECL. Blots were exposed to Bio Max MR films and quantified using Image Quant software, version 5.2 (GE Healthcare).

Plasma lipase activity

Lipase activity was determined in pre- and postheparin plasma (32). After fasting for 4 h, blood was harvested from mice. Then heparin (100 units/kg body weight) was injected via a tail vein. After 5 min, blood was obtained by retro-orbital bleeding, and plasma was frozen at -80°C . Pre- and postheparin plasma lipase activity were assayed using an artificial glycerol tri- $[1-^{14}\text{C}]$ oleate-containing emulsion (33).

Adrenal cholesterol analysis

Mice were euthanized, and adrenal glands were harvested and immediately frozen (24). The glands were subsequently homogenized. Protein in the homogenates was measured using the method described by Lowry et al. (34). Cholesterol was analyzed with a commercial fluorometric assay. Cholesterol content is expressed as μg cholesterol/mg protein.

Miscellaneous

Routinely, all mice were fasted for 4 h before blood was harvested for analytical or preparative purposes. Total cholesterol,

unesterified cholesterol, HDL cholesterol, triglycerides, and phospholipids from plasma and lipoproteins were measured using commercial enzymatic assays. Plasma lipoproteins were fractionated by fast protein liquid chromatography (FPLC) (35). Protein was analyzed as outlined (34).

For determination of free fatty acids, tetrahydrolipstatin (THL, 25 µg/ml) was added to murine blood (36). THL prevents *in vitro* lipolysis of triglycerides, which could lead to an overestimation of fatty acids. Plasma free fatty acids were determined using a commercial kit, which was adapted to microtiter plates.

Statistics and calculations

Values are means ± SEM. All statistical analyses were performed using Student's *t*-test. Probability values less than 0.05 were considered statistically significant.

RESULTS

CD36, plasma lipids, and lipoproteins of mice

A targeted mutation in the gene encoding CD36 in mice induced an increase in plasma cholesterol (Table 1) (15, 16). Compared with WT mice, cholesterol increased by 33% in CD36 KO animals. To determine the lipoprotein fraction which was modified by the CD36 deficiency, FPLC was used (Fig. 1). Compared with WT mice, the increase in plasma cholesterol in CD36 KO littermates was predominantly due to a rise in the HDL fraction. Plasma HDL analysis was also performed by precipitation of apolipoprotein B-containing lipoproteins and subsequent cholesterol measurement in the supernatant (Table 1). Compared with WT mice, HDL cholesterol of CD36 KO animals increased by 37%.

CD36 can facilitate the cellular uptake of fatty acids (10), and CD36 KO mice may show an increase in plasma triacylglycerol and fatty acids (15, 37). Therefore triglycerides and free fatty acids were measured in WT and in CD36 KO mice (Table 1). No significant differences in plasma triglycerides and fasting fatty acids were detected either in the absence or presence of CD36.

Following preparation from plasma, the chemical composition of WT-HDL and of CD36 KO-HDL was investigated (Table 2). This analysis revealed no significant differences between WT-HDL and CD36 KO-HDL.

CD36 and HDL metabolism in mice

To explore a possible mechanism of the CD36 deficiency-induced increase in HDL, we investigated whether this scavenger receptor has a role in HDL internalization and catabolism. Metabolic studies were performed using

murine HDL, which was radiolabeled in the protein (^{125}I -TC) as well as in the CE ($[^3\text{H}]\text{CEt}$) moiety (2, 9). HDL apolipoprotein-associated ^{125}I -TC represents the metabolism of HDL holo-particles, and the difference between $[^3\text{H}]\text{CEt}$ and ^{125}I -TC yields selective CE uptake from HDL (38).

^{125}I -TC/ $[^3\text{H}]\text{CEt}$ -HDL was injected in WT and CD36 KO mice (Fig. 2A). Over a 24 h, periodic blood samples were collected for analysis of ^{125}I -TC and $[^3\text{H}]\text{CEt}$. In WT animals, the plasma decay of HDL-associated $[^3\text{H}]\text{CEt}$ was faster than that of ^{125}I -TC. The difference between $[^3\text{H}]\text{CEt}$ and ^{125}I -TC yields selective CE clearance from HDL in controls (2). In CD36 KO mice, the decay of ^{125}I -TC was decreased compared with WT, suggesting a reduced rate of HDL holo-particle catabolism. In CD36 KO mice, selective CE removal ($[^3\text{H}]\text{CEt} - ^{125}\text{I}$ -TC) from plasma HDL was diminished compared with WT rodents.

Plasma FCRs were calculated (2, 22) from HDL decay curves (Fig. 2A). In WT mice, the plasma FCR for HDL-associated $[^3\text{H}]\text{CEt}$ was higher than that for ^{125}I -TC (Fig. 2B). The difference in plasma FCRs ($[^3\text{H}]\text{CEt} - ^{125}\text{I}$ -TC) yields selective CE clearance from plasma HDL by tissues, and the respective rate was substantial in WT mice (9). In CD36 KO animals, a decrease of 28% in plasma FCR for ^{125}I -TC was observed, which suggests a reduction in HDL holo-particle catabolism compared with WT (corresponding to 100%). Selective CE removal from circulating HDL ($[^3\text{H}]\text{CEt} - ^{125}\text{I}$ -TC) was significantly diminished by 29% in CD36 KO animals compared with WT (corresponding to 100%).

To investigate the function of CD36 in tissue HDL metabolism, mice were euthanized 24 h after ^{125}I -TC/ $[^3\text{H}]\text{CEt}$ -HDL injection, and tissues were harvested for tracer content analysis (2). Based on plasma FCRs and fractional tracer recovery of individual tissues, the organ FCRs for each HDL tracer were calculated. These organ FCRs represent the fraction of the plasma pool of the traced HDL component cleared by a tissue per h.

For the liver of WT mice, the organ FCR for HDL-associated $[^3\text{H}]\text{CEt}$ was higher than the respective rate for ^{125}I -TC (Fig. 3A). Selective HDL CE uptake ($[^3\text{H}]\text{CEt} - ^{125}\text{I}$ -TC) by the liver was substantial compared with hepatic HDL holo-particle internalization (^{125}I -TC) in WT animals (9). In contrast, in CD36 KO mice, the hepatic organ FCR for HDL-associated ^{125}I -TC decreased by 29% compared with WT, which suggests a decline in HDL holo-particle uptake by the mutant liver (Fig. 3A). In the CD36-deficient liver, the organ FCR for $[^3\text{H}]\text{CEt}$ was reduced by 32% and selective CE uptake from HDL ($[^3\text{H}]\text{CEt} - ^{125}\text{I}$ -TC) was diminished by 33% (WT corresponds to 100%).

TABLE 1. Plasma cholesterol, HDL cholesterol, triglycerides, and fatty acids of WT and CD36 KO mice

	Total Cholesterol	HDL Cholesterol	Triglyceride	Fatty Acid
	mg/dl	mg/dl	mg/dl	mg/dl
Wildtype	89.2 ± 3.0 (27)	56.0 ± 6.9 (8)	108.9 ± 8.4 (14)	11.0 ± 1.5 (7)
CD36 KO	119.0 ± 7.7 (32)	76.6 ± 3.1 (8)	111.8 ± 8.4 (16)	11.0 ± 2.2 (4)
<i>P</i>	0.001	0.008	0.81	0.99

Male mice were fasted for 4 h. Then blood was harvested and plasma was analyzed as outlined in "Materials and Methods." Values are means ± SEM. The number of mice is given in parentheses.

CD36, cluster of differentiation 36; KO, knockout; WT, wildtype.

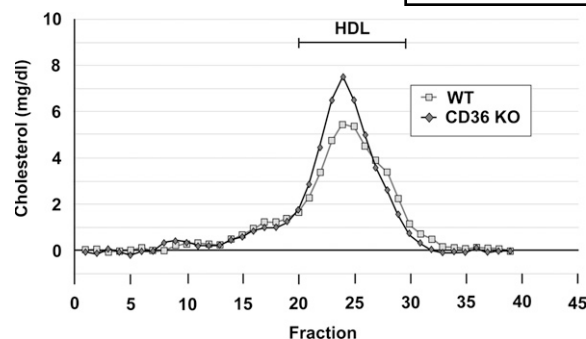


Fig. 1. FPLC analysis of plasma cholesterol from WT and CD36 KO mice. After fasting for 4 h, blood was harvested from three WT and three CD36 KO male mice. The pooled plasma was subjected to FPLC, and cholesterol was analyzed in each fraction. Shown is a representative experiment from a total of $n = 3$. CD36, cluster of differentiation 36; FPLC, fast protein liquid chromatography; KO, knockout; WT, wildtype.

$^{125}\text{I-TC-}/[{}^3\text{H}]\text{CEt-HDL}$ uptake by adrenals in WT mice revealed a higher organ FCR for $[{}^3\text{H}]\text{CEt}$ compared with $^{125}\text{I-TC}$, and selective CE uptake ($[{}^3\text{H}]\text{CEt} - ^{125}\text{I-TC}$) was substantial in normal glands compared with HDL holo-particle ($^{125}\text{I-TC}$) internalization (Fig. 3B) (9). In adrenals from CD36 KO mice, the organ FCRs for $^{125}\text{I-TC}$ and $[{}^3\text{H}]\text{CEt}$ decreased by 37% and 40%, respectively. This decline indicated a decrease of 37% of HDL holo-particle uptake and yielded a significant reduction of 41% of selective CE uptake ($[{}^3\text{H}]\text{CEt} - ^{125}\text{I-TC}$) by adrenal glands from CD36-deficient mice compared with WT (corresponding to 100%). In summary, these experiments provide evidence for a role of CD36 in hepatic and adrenal HDL metabolism.

$^{125}\text{I-TC-}/[{}^3\text{H}]\text{CEt-HDL}$ uptake by nonhepatic and non-steroidogenic tissues was explored. In kidneys of WT mice, the organ FCR for HDL-associated $^{125}\text{I-TC}$ was higher than the rate for $[{}^3\text{H}]\text{CEt}$; this result is consistent with a role of these organs in HDL apolipoprotein catabolism (Fig. 3C) (39). In kidneys of CD36 KO animal, the organ FCR for HDL-associated $^{125}\text{I-TC}$ decreased by 35%; this observation is line with a role of CD36 in renal HDL apolipoprotein catabolism. Kidney organ FCRs for HDL-associated $[{}^3\text{H}]\text{CEt}$ were similar in WT and CD36 KO mice.

TABLE 2. Chemical composition of murine HDL

	WT-HDL	CD36 KO-HDL	<i>P</i>
	% Total Mass	% Total Mass	
Unesterified cholesterol	2.16 ± 0.30	1.76 ± 0.33	0.276
Esterified cholesterol	7.82 ± 0.70	6.74 ± 0.98	0.086
Phospholipid	15.5 ± 0.95	13.6 ± 1.08	0.266
Triglyceride	0.575 ± 0.094	0.500 ± 0.083	0.519
Protein	73.0 ± 1.1	77.4 ± 1.9	0.110

Blood was harvested in parallel from fasted (4 h) WT and CD36 KO male mice. Then HDL ($d = 1.063\text{-}1.21$ g/ml) was isolated from plasma by sequential ultracentrifugation. Total cholesterol, unesterified cholesterol, phospholipids, triglycerides, and protein were analyzed. Esterified cholesterol was calculated as difference between total and unesterified cholesterol. Values are means ± SEM of $n = 5$ independent preparations. Analysis was carried out in duplicate or triplicate in each sample.

CD36, cluster of differentiation 36; KO, knockout; WT, wildtype.

Uptake of $^{125}\text{I-TC-}/[{}^3\text{H}]\text{CEt-HDL}$ by spleen, stomach, intestine, brain, heart, lungs, and carcass was investigated (supplementary Table I). Compared with the liver, the organ FCRs for all tissues except carcass were quantitatively small. This result reinforces a dominant role of the liver in HDL catabolism in mice (2, 9). In WT rodents, some selective CE uptake ($[{}^3\text{H}]\text{CEt} - ^{125}\text{I-TC}$) from HDL was detected in spleen, stomach, brain, heart, lungs, and carcass. In the intestine of WT mice, no selective CE uptake from HDL was measured. In CD36 KO animals, selective HDL CE uptake declined significantly in spleen, stomach, brain, and lungs compared with WT controls.

CD36 and HDL metabolism of hepatocytes and of nonparenchymal liver cells

The liver is composed of distinct cell populations, including hepatocytes, KCs, and LSECs (40). Differences in HDL metabolism of specific hepatic cell fractions have been established (6). To investigate whether the regulation of HDL uptake by the CD36-deficient liver is due to a decrease of the respective pathways in distinct cell populations, HDL metabolism was explored in both primary hepatocytes and nonparenchymal liver cells (9). The cells were prepared from WT or CD36 KO mice (23, 26). After culturing, cells were incubated in medium containing $^{125}\text{I-TC-}/[{}^3\text{H}]\text{CEt-HDL}$. The cellular tracer content was analyzed and expressed in terms of apparent HDL particle uptake (2, 25).

Murine hepatocytes were incubated in medium containing $^{125}\text{I-TC-}/[{}^3\text{H}]\text{CEt-HDL}$ (Fig. 4). In WT cells, apparent HDL particle uptake according to $^{125}\text{I-TC}$ increased as the HDL concentration in the medium rose. Apparent HDL particle uptake due to $[{}^3\text{H}]\text{CEt}$ was in excess of that according to $^{125}\text{I-TC}$, and this lipid uptake increased in a dose-dependent manner throughout the entire concentration range. Apparent selective CE uptake ($[{}^3\text{H}]\text{CEt} - ^{125}\text{I-TC}$) rose in hepatocytes from WT mice as a function of the HDL concentration. Uptake of $^{125}\text{I-TC-}/[{}^3\text{H}]\text{CEt-HDL}$ was explored in CD36 KO hepatocytes in parallel. In CD36-deficient cells, apparent HDL particle uptake according to $^{125}\text{I-TC}$ was dose-dependent, and this uptake decreased by 18-27% compared with WT hepatocytes (set as 100%). In mutant hepatocytes, apparent HDL particle uptake according to $[{}^3\text{H}]\text{CEt}$ was reduced by 21-26% throughout the HDL concentration range. Apparent selective HDL CE uptake ($[{}^3\text{H}]\text{CEt} - ^{125}\text{I-TC}$) was diminished by 21-30% in CD36-deficient hepatocytes compared with WT cells.

SR-BI KO-HDL yields a lower rate of selective CE uptake compared with WT-HDL in vitro (9). To address whether radiolabeled WT-HDL or CD36 KO-HDL yields similar or different rates of HDL uptake in primary murine liver cells, primary hepatocytes were isolated from WT mice. The cells were incubated (37°C, 2.0 h) in medium containing $^{125}\text{I-TC-}/[{}^3\text{H}]\text{CEt-WT-HDL}$ (40 µg HDL protein/ml) or $^{125}\text{I-TC-}/[{}^3\text{H}]\text{CEt-CD36 KO-HDL}$ (40 µg HDL protein/ml). Apparent HDL holo-particle uptake ($^{125}\text{I-TC}$) was not significantly different between both HDL preparations (data not shown). Analogously, selective HDL CE uptake ($[{}^3\text{H}]\text{CEt} - ^{125}\text{I-TC}$) was not significantly different between both radiolabeled HDL preparations (data not shown).

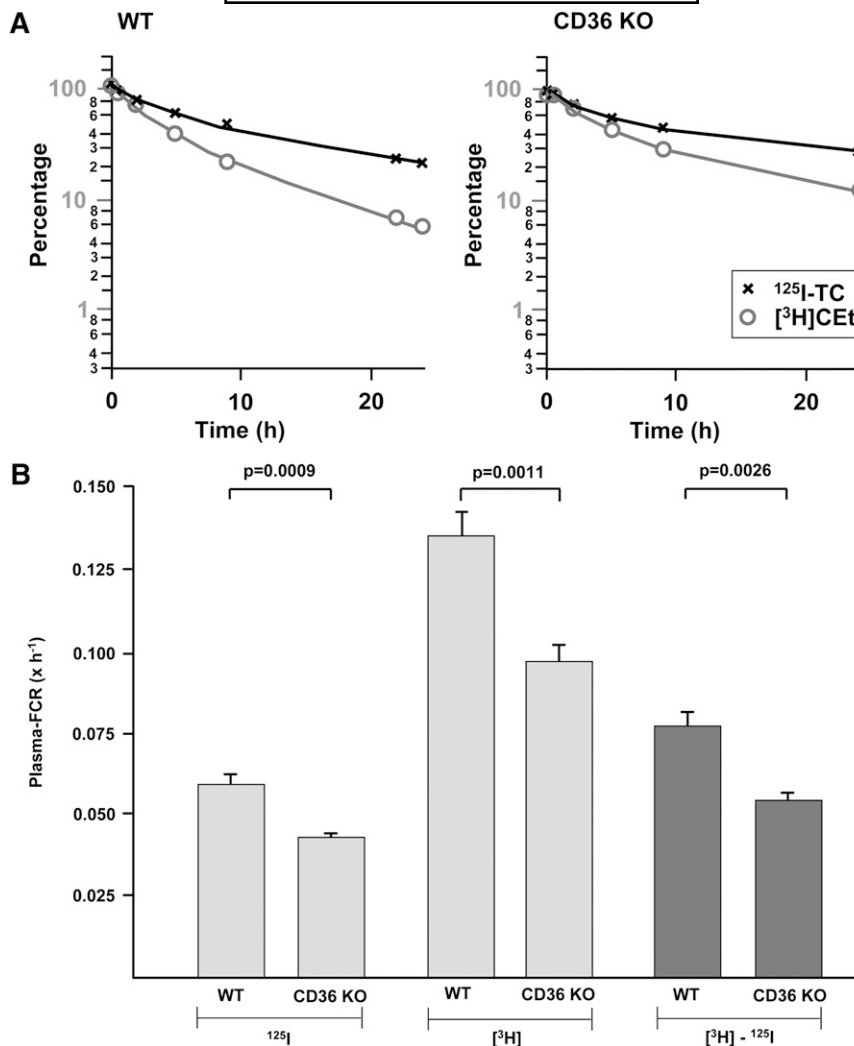


Fig. 2. Plasma decay kinetics and plasma FCRs of ¹²⁵I-TC-/[³H]CEt-HDL in WT and CD36 KO mice. ¹²⁵I-TC-/[³H]CEt-HDL was injected intravenously in WT or in parallel in CD36 KO male mice. Then periodic blood samples were collected over 24 h, and plasma was analyzed for ¹²⁵I-TC and [³H]CEt. A: One representative experiment of n = 10 (WT) and n = 10 (CD36 KO) mice. B: Plasma FCRs for each tracer for each mouse were calculated from the decay curves shown in Fig. 2A. ¹²⁵I represents ¹²⁵I-TC, [³H] shows [³H]CEt, and [³H] - ¹²⁵I indicates selective CE metabolism. Results are means ± SEM of n = 10 (WT) and n = 10 (CD36 KO) mice. CD36, cluster of differentiation 36; CE, cholesteryl ester; CEt, cholesteryl oleyl ether; FCR, fractional catabolic rate; KO, knockout; TC, tyramine cellobiose; WT, wildtype.

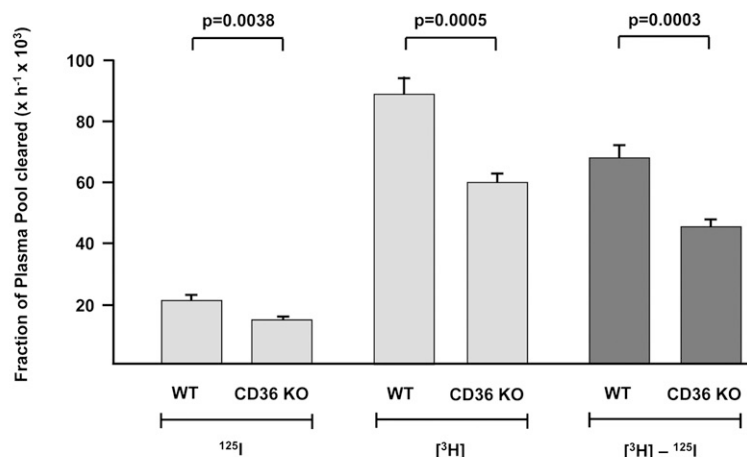
The metabolism of ¹²⁵I-TC-/[³H]CEt-HDL was investigated in primary nonparenchymal liver cells (Fig. 5). In cells from WT mice, apparent HDL particle uptake according to [³H]CEt was higher compared with ¹²⁵I-TC, and the difference between both tracers yields apparent selective CE uptake ([³H]CEt - ¹²⁵I-TC). In nonparenchymal hepatic cells from CD36 KO mice, apparent HDL particle uptake according to ¹²⁵I-TC and [³H]CEt decreased by 8% and 25%, respectively, and this decline yielded a decrease of 31% for selective CE uptake (WT corresponds to 100%). Remarkably, based on cell protein, nonparenchymal hepatic cells quantitatively had a higher rate of HDL uptake compared with hepatocytes.

In summary, these experiments suggest a role for CD36 in both hepatocytes and in nonparenchymal hepatic cells for HDL metabolism.

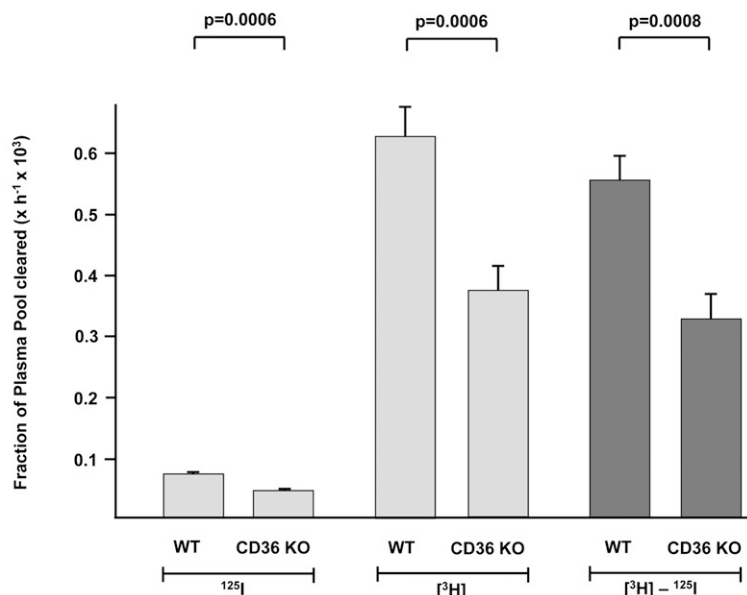
Adenovirus-mediated CD36 expression and HDL metabolism in vitro

In the experiments described above, mice or cells with a deficiency of CD36 were the model. Next the effect of a high CD36 expression on cellular HDL internalization was determined. CD36 expression was induced with a recombinant adenovirus which encodes murine CD36 (Ad-mCD36) (27, 28). H1299 cells were incubated in medium containing no virus (mock), Ad-GFP (control), or Ad-mCD36 (Fig. 6). After cell harvest, CD36 expression in postnuclear supernatants from these cells was explored by immunoblotting. Ad-mCD36 induced a substantial expression of CD36 in H1299 cells; in contrast, this scavenger receptor was not detected in cells incubated without virus (mock) or with Ad-GFP. Thus, cells with significant CD36 expression or with no immunodetectable CD36 were available.

A Liver



B Adrenals



C Kidneys

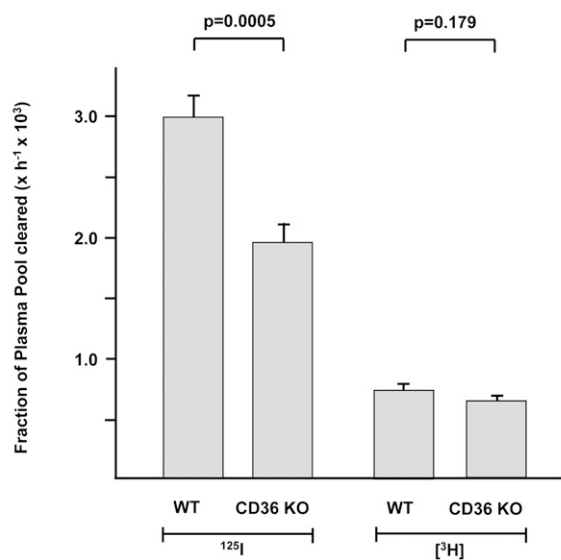


Fig. 3. Liver (A), adrenal (B), and kidney (C) FCRs for ¹²⁵I-TC-/[³H]CEt-HDL in WT and CD36 KO mice. ¹²⁵I-TC-/[³H]CEt-HDL was injected intravenously in WT and CD36 KO male mice. During the subsequent 24 h interval, periodic blood samples were harvested, and plasma was analyzed for ¹²⁵I-TC and [³H]CEt. From these results, plasma FCRs for each tracer were calculated. At 24 h after injection, the animals were euthanized, organs were harvested, and tracer uptake was analyzed. Organ FCRs were calculated as described in “Materials and Methods.” ¹²⁵I represents ¹²⁵T-TC, [³H] shows [³H]CEt, and [³H] - ¹²⁵I indicates selective CE metabolism. Results are means ± SEM of n = 10 (WT) and n = 10 (CD36 KO) mice. Tissue analysis was carried out in duplicate in each animal. CD36, cluster of differentiation 36; CE, cholesteryl ester; CEt, cholesteryl oleyl ether; FCR, fractional catabolic rate; KO, knockout; TC, tyramine cellobiose; WT, wildtype.

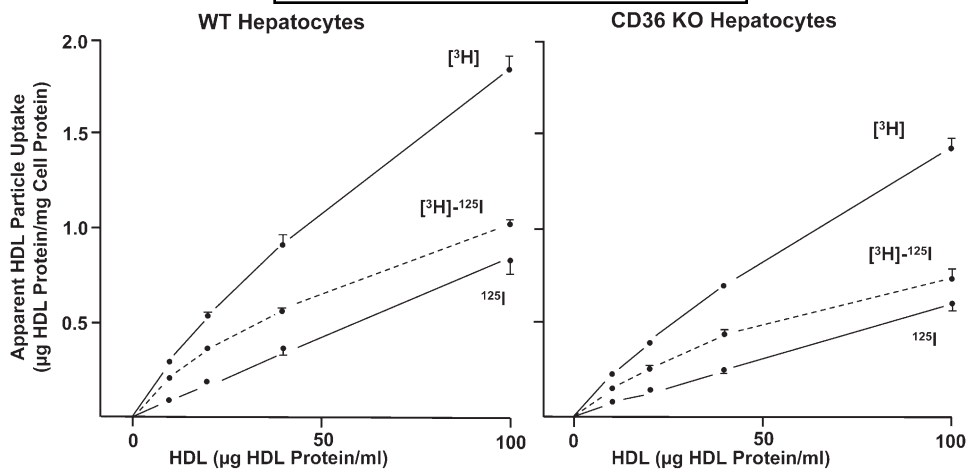


Fig. 4. Uptake of ^{125}I -TC-/ ^3H]CEt-HDL by hepatocytes isolated from WT and CD36 KO mice. Hepatocytes were prepared from male WT and CD36 KO mice. After culture, cells were incubated (37°C , 2 h) in medium containing ^{125}I -TC-/ ^3H]CEt-HDL (the respective concentrations are indicated on the X axis). The tracer uptake was analyzed as described in "Materials and Methods." ^{125}I represents ^{125}I -TC, ^3H shows ^3H]CEt, and ^3H - ^{125}I indicates selective CE uptake. Values are means \pm SEM of $n = 3$ experiments. Incubations were carried out in duplicate in each experiment. Where no error bars are shown, the SEM was smaller than the respective point. For comparison of ^{125}I -TC uptake between WT and CD36 KO, P values were between 0.0135 and 0.031; for comparison of ^3H]CEt uptake between both groups, P values were between 0.0023 and 0.031; for comparison of ^3H]CEt - ^{125}I -TC uptake between WT and CD36 KO, P values were between 0.007 and 0.0099. CD36, cluster of differentiation 36; CE, cholesteryl ester; CET, cholesteryl oleyl ether; FCR, fractional catabolic rate; KO, knockout; TC, tyramine cellobiose; WT, wildtype.

To address whether CD36 mediates HDL uptake in vitro, H1299 cells were cultured in medium containing no virus (mock), Ad-GFP (control), or Ad-mCD36 (Fig. 7). Then the cells were incubated in the presence of ^{125}I -TC-/ ^3H]CEt-HDL, and the HDL tracer uptake was analyzed. Compared with Ad-GFP, Ad-mCD36 induced an increase of 694% in apparent HDL particle uptake (^{125}I -TC) in H1299 cells. Compared with Ad-GFP, Ad-mCD36 stimulated apparent HDL particle uptake according to ^3H]CEt significantly (by 249%). In relation to Ad-GFP, Ad-mCD36 induced a 209% increase in selective CE uptake (^3H]CEt - ^{125}I -TC) from HDL. Compared with control (mock, DMEM), virus Ad-GFP quantitatively had only a minor effect on HDL uptake by H1299 cells.

Next the effect of CD36 on the dose response curve for HDL uptake in H1299 cells was explored (supplementary Fig. 1). Again, H1299 cells were kept in the medium containing no virus (mock), Ad-GFP, or Ad-mCD36. Following incubation of the cells in the presence of ^{125}I -TC-/ ^3H]CEt-HDL, the respective concentration range was 10-100 μg HDL protein/ml. Compared with Ad-GFP, Ad-mCD36 induced an increase in apparent HDL particle uptake according to ^{125}I -TC throughout the entire concentration range of HDL. Analogously, Ad-mCD36 induced an increase in apparent selective CE uptake (^3H]CEt - ^{125}I -TC) throughout the entire concentration range of HDL compared with Ad-GFP.

In summary, the expression of CD36 substantially stimulates apparent HDL holo-particle internalization (^{125}I -TC)

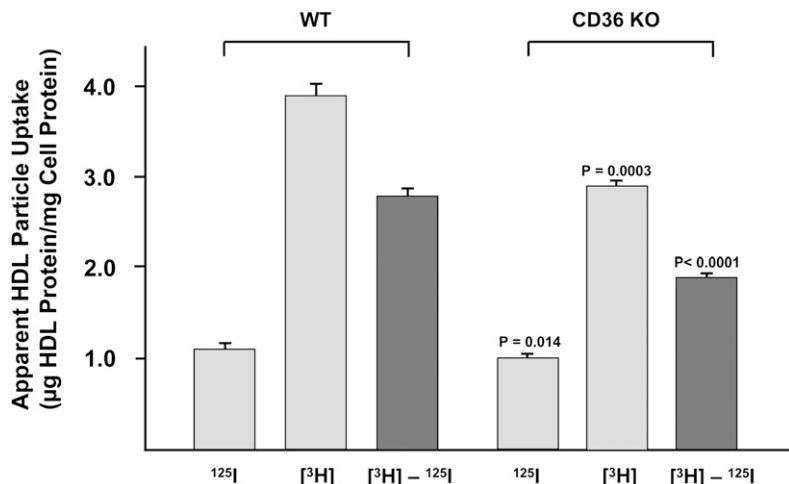


Fig. 5. Uptake of ^{125}I -TC-/ ^3H]CEt-HDL by nonparenchymal cells of the liver isolated from WT and CD36 KO mice. Nonparenchymal cells were prepared from male mice. After culture, cells were incubated (37°C , 2.0 h) in medium containing ^{125}I -TC-/ ^3H]CEt-HDL (40 μg HDL protein/ml). The tracer uptake was analyzed as described in "Materials and Methods." ^{125}I represents ^{125}I -TC, ^3H shows ^3H]CEt, and ^3H - ^{125}I indicates selective CE uptake. Values are means \pm SEM of $n = 5$ (WT) and $n = 3$ (CD36 KO) independent experiments. Incubations were carried out in triplicate in each experiment. CD36, cluster of differentiation 36; CE, cholesteryl ester; CET, cholesteryl oleyl ether; FCR, fractional catabolic rate; KO, knockout; TC, tyramine cellobiose; WT, wildtype.

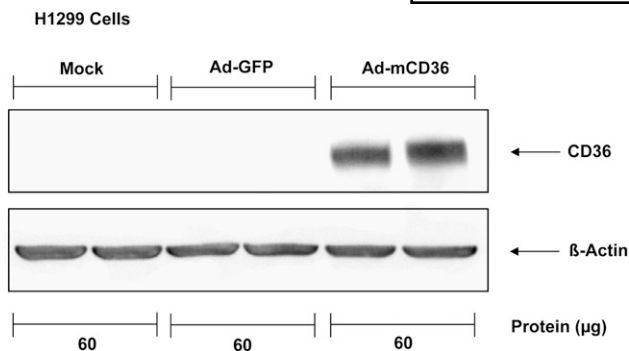


Fig. 6. Adenovirus-mediated CD36 expression in H1299 cells. H1299 cells incubated (37°C, 72 h) in medium containing no virus (mock, DMEM), Ad-GFP (MOI 200), or Ad-mCD36 (MOI 200). Then postnuclear supernatants were prepared from these cells. The proteins were subjected to electrophoresis followed by transfer to a membrane. Then the proteins were immunoblotted using CD36- or β -actin-specific antibodies. Shown is a typical blot; three independent experiments yielded qualitatively identical results. CD36, cluster of differentiation 36

as well as selective CE uptake from HDL under the experimental conditions of this study.

SR-BI, LRP1, and CD36 expression in murine liver, hepatocytes, and adrenal glands

As described above, HDL uptake was diminished in the liver and adrenals of CD36 KO mice. SR-BI and, presumably, low density lipoprotein receptor-related protein 1

(LRP1) mediate selective CE uptake by tissues (3, 41). With respect to molecular mechanism(s), we wondered whether the decrease in HDL uptake in CD36 KO mice was due to the deletion of this scavenger receptor per se or, alternatively, whether a CD36-mediated downregulation of SR-BI and/or of LRP1 was involved. To investigate this, the expression of SR-BI, LRP1, and CD36 was determined in membranes isolated from murine liver and adrenals. To ensure that these receptors were expressed by hepatocytes per se, postnuclear supernatants from primary hepatocytes were also prepared and probed for the respective receptors.

In liver membranes from WT and CD36 KO mice, SR-BI expression was identical in both membranes according to immunoblots (Fig. 8A). As expected, in membranes prepared from CD36 KO liver, no CD36 signal was observed, whereas the respective band was detected in WT proteins (Fig. 8B). CD36 expression was visible in these blots in murine peritoneal macrophages, which were included as reference for CD36 (5). To investigate SR-BI in liver parenchymal cells, postnuclear supernatants were prepared from hepatocytes isolated from WT and CD36 KO mice (Fig. 8C). SR-BI expression in these immunoblots was identical in hepatocyte proteins isolated from WT and CD36 KO mice. However, a signal for CD36 was detected only in postnuclear supernatants isolated from WT hepatocytes.

To address whether a downregulation of LRP1 was responsible for the reduced HDL uptake of CD36 KO mice, liver membranes and hepatocyte postnuclear supernatants

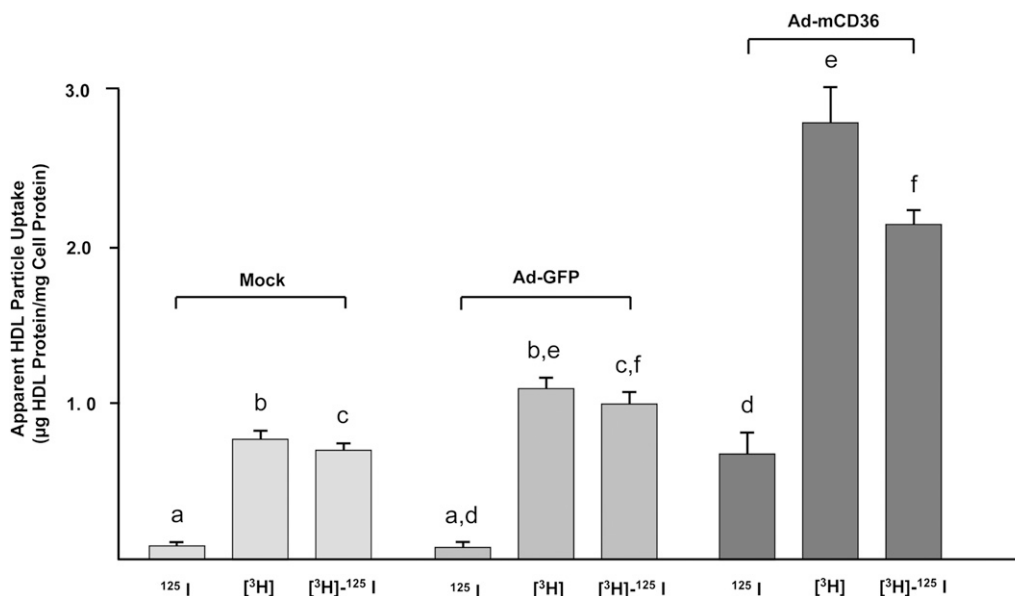


Fig. 7. Effect of adenovirus-mediated CD36 expression on uptake of ^{125}I -TC/ ^3H CEt-HDL by H1299 cells. H1299 cells incubated (37°C, 72 h) in medium containing no virus (mock, DMEM), Ad-GFP (MOI 200), or Ad-mCD36 (MOI 200). After culture, cells were incubated (37°C, 4.0 h) in medium containing ^{125}I -TC/ ^3H CEt-HDL (40 μg HDL protein/ml). Finally cellular tracer uptake was analyzed. ^{125}I represents ^{125}I -TC, ^3H shows ^3H CEt, and ^3H - ^{125}I (^3H CEt - ^{125}I -TC) represents apparent selective CE uptake from HDL. Values are means \pm SEM of $n = 3$ independent experiments. In each experiment, triplicate independent determinations were made. $P = 0.5$ (A); $P = 0.006$ (B); $P = 0.005$ (C); $P = 0.003$ (D); $P < 0.0001$ (E); and $P < 0.0001$ (F). CD36, cluster of differentiation 36; CE, cholesteryl ester; CEt, cholesteryl oleyl ether; MOI, multiplicity of infection; TC, tyramine cellobiose.

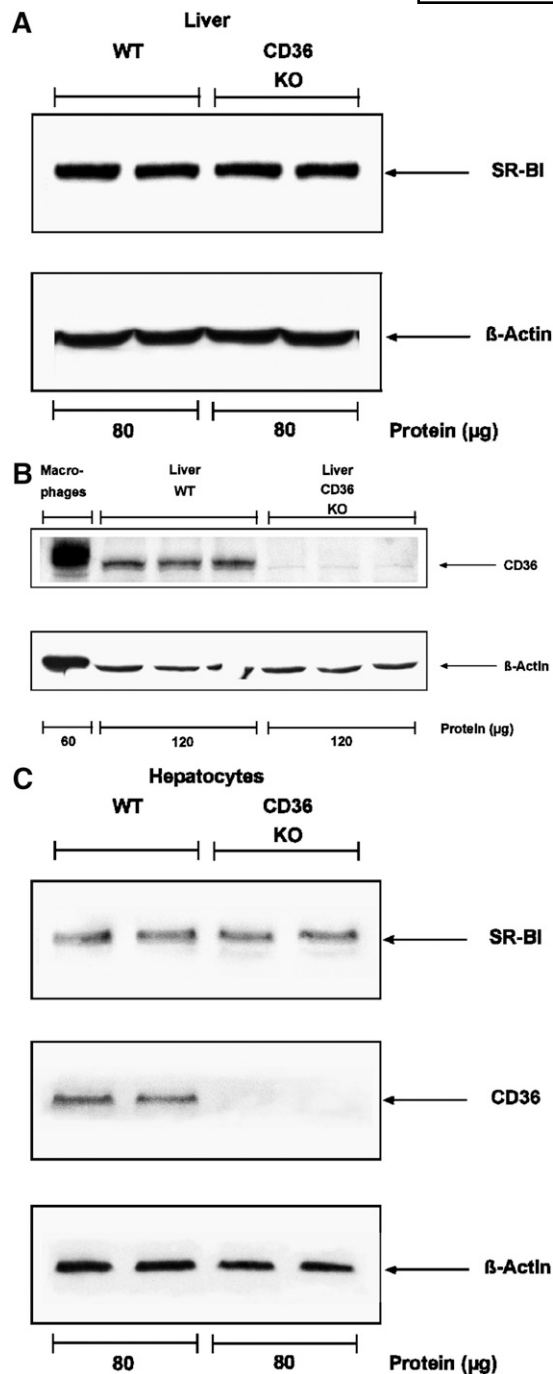


Fig. 8. SR-BI and CD36 expression in liver membranes and post-nuclear supernatants prepared from hepatocytes isolated from WT or from CD36 KO mice. **A, B:** Membrane fractions were isolated from livers of WT and CD36 KO male mice. As reference for CD36, a postnuclear supernatant was prepared from WT murine peritoneal macrophages (**B**). **C:** Hepatocytes were isolated from WT and CD36 KO male mice. After culture (37°C, 2.0 h), postnuclear supernatants were prepared from these cells. The indicated mass of protein was subjected to electrophoresis and transferred to a membrane. The proteins were immunoblotted using SR-BI-, CD36-, or β -actin-specific antibodies. β -actin was used as loading control. Typical blots are shown; four (**A**), three (**B**), or three (**C**) independent blots yielded qualitatively identical results. CD36, cluster of differentiation 36; KO, knockout; SR-BI, scavenger receptor class B type I; WT, wildtype.

were prepared from WT and CD36 KO mice (**Fig. 9**) (41). Immunoblots showed no difference in LRP1 expression in both groups of proteins from murine liver or hepatocytes.

In murine adrenals, immunoblots yielded an identical signal for SR-BI in membranes prepared from WT and CD36 KO mice (**Fig. 10**). In contrast, CD36 expression was detected only in adrenal membranes isolated from WT mice (data not shown).

In summary, SR-BI and LRP1 expression were identical in liver of WT and of CD36 KO mice, and the same was true for SR-BI in adrenal glands. These results imply that in the liver a deficiency of CD36 is responsible for the decreased HDL uptake observed in this organ in vivo.

Lipase activity and HDL metabolism

Lipoprotein lipase can stimulate selective HDL CE uptake independent from lipolysis (42). In CD36-deficient mice, LPL-mediated hydrolysis of lipoproteins was decreased compared with WT animals (37). Therefore, it could be that differences in HDL metabolism between WT and CD36 KO mice were due to variations in LPL activity. To investigate this, lipase activity was analyzed in WT and CD36 KO mice (**Table 3**). No difference in pre- and post-heparin plasma lipase activity was detected between mice with and without CD36 expression.

CD36 and adrenal gland cholesterol

HDL delivers cholesterol to adrenals as substrate for steroid hormone synthesis (38, 43). Analyzed with an isotope approach, in adrenals from CD36 KO mice, HDL uptake decreased compared with the respective HDL internalization of WT glands (**Fig. 3B**). To address the role of CD36 for HDL-mediated adrenal lipid accumulation in more detail, cholesterol mass was analyzed in glands from WT and mutant mice (**Table 3**). Total cholesterol mass decreased by 22% in glands isolated from CD36 KO mice compared with WT adrenals (corresponding to 100%). This result reinforces a physiological role of CD36 for HDL-mediated cholesterol delivery to tissues.

DISCUSSION

A major effect of CD36 deficiency in mice is an increase in plasma cholesterol; this change in phenotype is primarily due to a rise in HDL cholesterol. In this study, HDL cholesterol increased by 37% in CD36 KO mice. In previous investigations, a 33% increase in this lipoprotein fraction (15) and a 34% increase in total plasma cholesterol (16) were observed. This consistent change in HDL steady-state level is in agreement with a physiologic function of CD36 in HDL metabolism in vivo. Plasma triacylglycerol and fatty acids were not different between CD36 KO and WT animals in this study; this observation is in contrast to a previous report (15) but in agreement with another study (11). However, mouse strain-related genetic differences and specific experimental conditions (like diet) presumably explain the discrepancy.

Both HDL biosynthesis and HDL catabolism yield the steady state-level of this lipoprotein fraction in plasma.

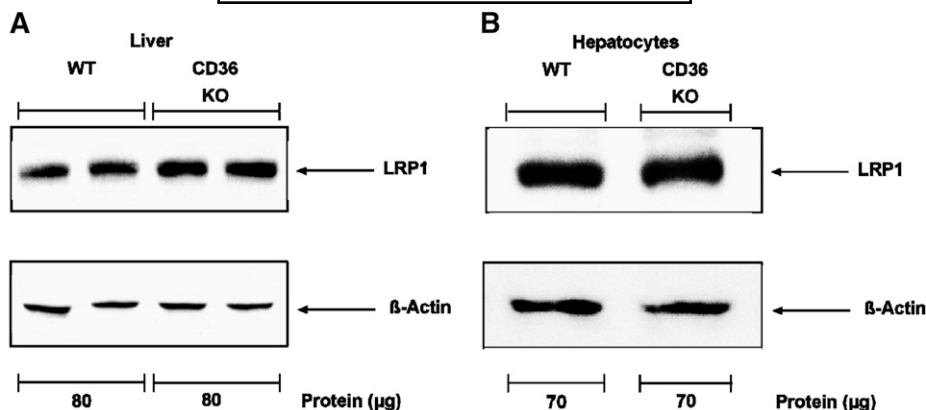


Fig. 9. LRP1 expression in liver membranes and postnuclear supernatants prepared from hepatocytes isolated from WT and CD36 KO mice. **A:** Membrane fractions were isolated from livers of WT and CD36 KO male mice. **B:** Hepatocytes were isolated from WT and CD36 KO male mice. After culture (37°C, 2.0 h), postnuclear supernatants were prepared from these cells. The proteins were subjected to electrophoresis and transferred to a membrane. Then the proteins were immunoblotted using LRP1- or β -actin-specific antibodies. Shown is a typical blot; one independent experiment yielded qualitatively identical results in each case. CD36, cluster of differentiation 36; KO, knockout; LRP1, low density lipoprotein receptor-related protein 1; WT, wildtype.

A recent investigation suggested that a deficiency of CD36 in mice is associated with an increase in HDL formation that finally yields an increase in HDL cholesterol (16). CD36 and SR-BI have a similar structure (4, 13), and the latter scavenger receptor has a major role in cellular HDL uptake and catabolism in vivo (8, 9). A function of CD36 in HDL uptake has been proposed on the basis of in vitro experiments; however, the lipid transfer rate of this protein may be lower compared with SR-BI (12, 13). In view of these observations, the hypothesis emerged that CD36 may have a role in HDL uptake and catabolism in vivo, analogous to SR-BI. We examined this hypothesis in mice and in liver and adrenals, the tissues of primary interest.

To explore the role of CD36 in HDL catabolism, a technique was employed that tracks the fate of distinct HDL components independently (2, 19). Using protein- and

lipid-labeled murine HDL, HDL holo-particle (125 I-TC) catabolism from the HDL plasma pool by tissues was detected in WT mice. Substantial selective CE removal from the HDL plasma pool by murine WT tissues was observed (9). As a major result of this study, a lack of CD36 reduced HDL holo-particle catabolism as well as selective CE clearance from HDL from the intravascular space. These data are in contrast to a recent study by Yue et al. (16) in CD36-deficient mice in which no effect of CD36 on HDL catabolism was suggested. However, several methodological differences between this and the other investigation (16) have to be considered. For example, Yue et al. (16) injected a huge mass of labeled HDL protein (180 μ g HDL protein per mouse), whereas here only a trace amount of this lipoprotein fraction was given (30 μ g HDL protein per mouse). Such a large mass of HDL increases the endogenous plasma pool of this lipoprotein fraction and thus may decrease the rate of HDL catabolism. This technical difference raises the question whether the experimental conditions of the other study (16) were physiologically appropriate.

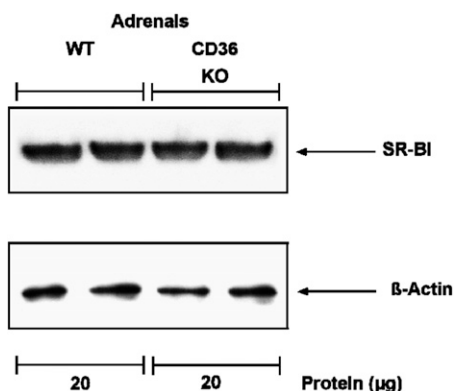


Fig. 10. SR-BI expression in adrenal membranes prepared from WT and CD36 KO mice. Membrane fractions were prepared from adrenals of WT and CD36 KO male mice. After electrophoresis and transfer to a membrane, the proteins were immunoblotted using SR-BI- or β -actin-specific antibodies. A typical blot is shown; two independent blots yielded qualitatively identical results. CD36, cluster of differentiation 36; KO, knockout; SR-BI, scavenger receptor class B type I; WT, wildtype.

TABLE 3. Lipase activity in plasma and adrenal gland cholesterol of WT and CD36 KO mice

Genotype	Lipase Activity		
	Pre-Heparin Plasma <i>mU/ml</i>	Post-Heparin Plasma <i>mU/ml</i>	Adrenal Gland Total Cholesterol μ g cholesterol/mg protein
WT	68.4 \pm 14.9 (6)	396.8 \pm 72.7 (6)	143.8 \pm 10.1 (10)
CD36 KO	63.5 \pm 9.0 (6)	375.9 \pm 89.0 (6)	112.1 \pm 6.9 (9)
<i>P</i>	0.94	0.36	0.0113

Blood was harvested from fasting (4 h) WT and CD36 KO male mice. Then heparin (100 units/kg body weight) was injected intravenously. Five min after injection, blood was harvested again. Pre- and postheparin lipase activity was measured in plasma as outlined in "Materials and Methods." Adrenals were harvested from male mice and analyzed for cholesterol and protein as described in "Materials and Methods." Values are means \pm SEM. The number of mice is indicated in parentheses.

CD36, cluster of differentiation 36; KO, knockout; WT, wildtype.

Besides plasma, the role of individual tissues for HDL catabolism was explored in this study. In WT mice, the liver quantitatively had the highest uptake rates for HDL holo-particles (^{125}I -TC) and for selective CE internalization. This result is consistent with a dominant role of this organ for HDL catabolism in vivo (2, 9). Adrenals showed the highest ratio of HDL lipid compared with protein uptake in WT rodents. HDL internalization by WT kidneys demonstrated a higher uptake of ^{125}I -TC compared with [^3H]Cet. This observation is in line with a preferential renal catabolism of HDL-associated apolipoproteins (39).

For tissue HDL metabolism of CD36-deficient mice, a really novel result from this investigation is a significant decline in selective HDL CE uptake by liver and adrenal glands compared with WT littermates. HDL holo-particle (^{125}I -TC) internalization by liver and adrenals was also significantly diminished in mutant rodents. This decreased HDL catabolism by organs of CD36-deficient mice provides evidence that CD36 mediates hepatic and adrenal HDL uptake and thus catabolism of this lipoprotein fraction. This diminished HDL uptake by tissues in CD36-deficient mice represents a mechanism that contributes to the increase of plasma HDL cholesterol of these mutant rodents. Remarkably, a recent study in CD36 mutant mice did not address the role of CD36 for HDL uptake by liver and adrenals in vivo (16). The physiologic relevance of CD36 for organ cholesterol homeostasis is underscored here by adrenal gland lipid mass analysis. In adrenals from CD36 KO mice, cholesterol mass declined significantly compared with WT. This observation also provides evidence for a function of CD36 in HDL-mediated cholesterol delivery to tissues.

The liver is composed of distinct cell populations, and only ~70% of all liver cells are parenchymal cells (i.e., hepatocytes) (40). HDL metabolism by defined hepatic cell types is heterogeneous (6). Due to this heterogeneity, the decreased hepatic HDL uptake in CD36 KO mice did not necessarily represent a decline in HDL catabolism by liver parenchymal cells per se. Alternatively, a decrease in HDL uptake by nonparenchymal hepatic cells could be the mechanism of the impairment of HDL uptake by the whole liver in CD36 KO animals. In this investigation, a CD36 deficiency significantly diminished selective HDL CE uptake and HDL holo-particle (^{125}I -TC) internalization by hepatocytes and nonparenchymal liver cells, and both results are in qualitative agreement with those obtained for the liver in vivo. Therefore, the decrease in HDL uptake observed in vivo must be attributed to a decline of these pathways in both hepatocytes and nonparenchymal liver cells. This observation is in contrast to results from Yue et al. (16) which suggested that a CD36 deficiency of murine hepatocytes had no role for hepatic HDL internalization. Again, substantial methodological differences have to be considered between that study (16) and this investigation. For example, in the other study, human HDL₃ (d = 1.125-1.21 g/ml) was radiolabeled with [^3H]cholesteryl oleyl ether, whereas here for HDL uptake analysis doubly-radiolabeled murine HDL (d = 1.063-1.21 g/ml) was applied. Only total HDL lipid uptake could be es-

timated by using [^3H]cholesteryl oleyl ether-labeled HDL₃ in the other study (16); a distinction between selective CE uptake and HDL particle internalization is not possible with this single isotope tracer. Besides, Yue et al. (16) used very high concentrations of radiolabeled HDL (100-300 μg HDL protein/ml) compared with this investigation, and such high HDL concentrations may be above saturation of the pathway. These technical differences presumably explain the discrepancy in results.


A possible role of CD36 for cellular HDL metabolism was explored in this study with a model in which this scavenger receptor was expressed using an adenovirus-mediated gene transfer. Ad-mCD36 induced a substantial expression of CD36 in cultured cells, and in parallel, Ad-mCD36 mediated an increase in HDL selective uptake and in HDL particle internalization. In contrast to these results, CD36 previously had a low efficiency for HDL uptake in cultured cells compared with SR-BI (12-14). A likely explanation for this discrepancy in results may be technical. Whereas in a previous study a plasmid vector was used for gene transfer, here an adenovirus was applied (13). Different methods for gene transfer may yield variations in the CD36 protein expression level. In addition, minor differences in the CD36 molecule structure may contribute to quantitative variations in HDL uptake efficiency of this scavenger receptor.

With respect to the molecular mechanisms responsible for the decrease in tissue HDL uptake in CD36 KO mice and CD36-deficient cells, several molecules, including SR-BI, LRP1 and LPL, may play a role (3, 41, 42). We considered whether regulation of these proteins occurred in CD36-deficient liver and cells that finally yielded the decrease in HDL uptake. Expression of SR-BI and LRP1 in liver and hepatocytes from WT and CD36 KO mice were identical in immunoblots. In adrenal glands, SR-BI expression in plasma membranes was identical in the presence and absence of CD36. Analogously, lipase activity in plasma was not different between both groups of animals. These results are in line with another study (16) and reinforce the concept that the inactivation of CD36 represents the mechanism responsible for the decrease in HDL uptake by tissues and the increase in plasma HDL cholesterol in CD36 KO mice.

SR-BI KO mice had an increase of 96% in plasma HDL cholesterol compared with WT littermates in a previous investigation (9). CD36 KO mice showed a rise of 37% in HDL cholesterol in this study. This comparison suggests that both SR-BI and CD36 have a function in HDL-mediated cholesterol delivery to tissues. However, on a quantitative basis, SR-BI has a major role in HDL metabolism and in tissue HDL uptake. With respect to specific organs, the expression of both SR-BI and CD36 in liver and adrenals are relevant for the regulation of plasma HDL cholesterol in mice.

In summary, a CD36 deficiency in mice significantly increases plasma HDL cholesterol (15, 16). One mechanism that contributes to this lipid increase is a decrease in HDL uptake by the liver and adrenals. In line with this observation in vivo, a lack of CD36 in hepatocytes and in

nonparenchymal liver cells in vitro diminished cellular HDL uptake. On the other hand, an adenovirus-mediated expression of CD36 stimulated HDL uptake by cells in vitro. Thus several lines of evidence show that CD36 has a role for cellular HDL uptake and catabolism. With respect to the increase in plasma HDL in CD36-deficient mice, an alternative mechanism has been suggested as well (16). Accordingly, a CD36 deficiency is associated with an increase in HDL formation in mice. However, results presented in both investigations are in line with the conclusion that presumably two mechanisms (i.e., increased HDL biosynthesis (16) and reduced HDL catabolism) contribute to the increase in steady-state plasma HDL cholesterol level in CD36-deficient mice.

CD36 has been implicated in the pathogenesis of atherosclerosis (4, 5). Initially this effect was attributed to a function of this scavenger receptor in the internalization of oxidatively modified lipoproteins by macrophages and subsequent lipid accumulation and foam cell formation in the arterial wall. However, recent studies point to a role of CD36 in the metabolism of native lipoproteins. This study and several others present evidence for a function of CD36 in HDL metabolism in mice (15, 16). Variations in the CD36 gene were implicated in the etiology of the metabolic syndrome in humans (44), and associations between variants in the gene of this receptor, HDL cholesterol levels, and the metabolic syndrome were identified. Evidence for a role of CD36 in the catabolism of native LDL in mice has been suggested as well (11). A function of CD36 in the clearance of fatty acid-enriched, triglyceride-rich particles (45) from plasma has been proposed, and intestinal CD36 has been involved in chylomicron formation (46). These results are in line with physiologic functions of CD36 in the metabolism of native lipoproteins. Thus, in addition to effects on the catabolism of modified particles, a role of CD36 in the metabolism of native lipoprotein fractions presumably contributes to the relationship between CD36 and atherosclerosis. 

The authors appreciate S. Ehret, B. Schulz, M. Thiel, and D. Evans for their assistance. R. E. Morton and D. J. Greene donated CETP, and U. J. F. Tietge supplied mice.

REFERENCES

- Von Eckardstein, A., J. R. Nofer, and G. Assmann. 2001. High density lipoproteins and arteriosclerosis. *Arterioscler. Thromb. Vasc. Biol.* **21**: 13–27.
- Glass, C., R. C. Pittman, M. Civen, and D. Steinberg. 1985. Uptake of high-density lipoprotein-associated apoprotein A-I and cholesterol esters by 16 tissues of the rat in vivo and by adrenal cells and hepatocytes in vitro. *J. Biol. Chem.* **260**: 744–750.
- Acton, S., A. Rigotti, K. T. Landschulz, S. Xu, H. H. Hobbs, and M. Krieger. 1996. Identification of scavenger receptor SR-BI as a high density lipoprotein receptor. *Science*. **271**: 518–520.
- Febbraio, M., and R. L. Silverstein. 2007. CD36: implications in cardiovascular disease. *Int. J. Biochem. Cell Biol.* **39**: 2012–2030.
- Endemann, G., L. W. Stanton, K. S. Madden, C. M. Bryant, R. T. White, and A. A. Protter. 1993. CD36 is a receptor for oxidized low density lipoprotein. *J. Biol. Chem.* **268**: 11811–11816.
- Out, R., M. Hoekstra, J. A. A. Spijkers, J. K. Kruijt, M. van Eck, I. S. T. Bos, J. Twisk, and T. J. C. van Berkel. 2004. Scavenger receptor class B type I is solely responsible for the selective uptake of cholesteryl esters from HDL by the liver and the adrenals in mice. *J. Lipid Res.* **45**: 2088–2095.
- Wang, N., T. Arai, Y. Ji, F. Rinninger, and A. R. Tall. 1998. Liver-specific overexpression of scavenger receptor BI decreases levels of very low density lipoprotein apoB, low density lipoprotein apoB, and high density lipoprotein in transgenic mice. *J. Biol. Chem.* **273**: 32920–32926.
- Rigotti, A., B. L. Trigatti, M. Penman, H. Rayburn, J. Herz, and M. Krieger. 1997. A targeted mutation in the murine gene encoding the high density lipoprotein (HDL) receptor scavenger receptor class B type I reveals its key role in HDL metabolism. *Proc. Natl. Acad. Sci. USA.* **94**: 12610–12615.
- Brundert, M., A. Ewert, J. Heeren, B. Behrendt, R. Ramakrishnan, H. Greten, M. Merkel, and F. Rinninger. 2005. Scavenger receptor class B type I mediates the selective uptake of high-density lipoprotein-associated cholesteryl esters by the liver in mice. *Arterioscler. Thromb. Vasc. Biol.* **25**: 143–148.
- Abumrad, N. A., M. R. El-Maghrabi, E. Z. Amri, E. Lopez, and P. A. Grimaldi. 1993. Cloning of a rat adipocyte membrane protein implicated in binding or transport of long-chain fatty acids that is induced during preadipocyte differentiation. *J. Biol. Chem.* **268**: 17665–17668.
- Luangrath, V., M. R. Brodeur, D. Rhainds, and L. Brissette. 2008. Mouse CD36 has opposite effects on LDL and oxidized LDL metabolism in vivo. *Arterioscler. Thromb. Vasc. Biol.* **28**: 1290–1295.
- Gu, X., B. Trigatti, S. Xu, S. Acton, J. Babbitt, and M. Krieger. 1998. The efficient cellular uptake of high density lipoprotein lipids via scavenger receptor class B type I requires not only receptor-mediated surface binding but also receptor-specific lipid transfer mediated by its extracellular domain. *J. Biol. Chem.* **273**: 26338–26348.
- Connelly, M. A., S. M. Klein, S. Azhar, N. A. Abumrad, and D. L. Williams. 1999. Comparison of class B scavenger receptors, CD36 and scavenger receptor BI (SR-BI), shows that both receptors mediate high density lipoprotein-cholesteryl ester selective uptake but SR-BI exhibits a unique enhancement of cholesteryl ester uptake. *J. Biol. Chem.* **274**: 41–47.
- De Villiers, W. J. S., L. Cai, N. R. Webb, M. C. de Beer, D. R. van der Westhuizen, and F. C. de Beer. 2001. CD36 does not play a direct role in HDL or LDL metabolism. *J. Lipid Res.* **42**: 1231–1238.
- Febbraio, M., N. A. Abumrad, D. P. Hajjar, K. Sharma, W. Cheng, S. F. A. Pearce, and R. L. Silverstein. 1999. A null mutation in murine CD36 reveals an important role in fatty acid and lipoprotein metabolism. *J. Biol. Chem.* **274**: 19055–19062.
- Yue, P., Z. Chen, F. Nassir, C. Bernal-Mizrachi, B. Finck, S. Azhar, and N. A. Abumrad. 2010. Enhanced hepatic apoA-I secretion and peripheral efflux of cholesterol and phospholipid in CD36 null mice. *PLoS ONE.* **5**: e9906.
- Moore, K. J., J. El Khoury, L. A. Medeiros, K. Terada, C. Geula, A. D. Luster, and M. W. Freeman. 2002. A CD36-initiated signaling cascade mediates inflammatory effects of beta-amyloid. *J. Biol. Chem.* **277**: 47373–47379.
- Havel, R. J., H. A. Eder, and J. H. Bragdon. 1955. The distribution and chemical composition of ultracentrifugally separated lipoproteins in human serum. *J. Clin. Invest.* **34**: 1345–1353.
- Pittman, R. C., and C. A. Taylor. 1986. Methods for assessment of tissue sites of lipoprotein degradation. *Methods Enzymol.* **129**: 612–628.
- Morton, R. E., and D. B. Zilversmit. 1983. Inter-relationship of lipids transferred by the lipid-transfer protein isolated from human lipoprotein-deficient plasma. *J. Biol. Chem.* **258**: 11751–11757.
- Dole, V. P. 1956. A relation between non-esterified fatty acids in plasma and the metabolism of glucose. *J. Clin. Invest.* **35**: 150–154.
- Le, N. A., R. Ramakrishnan, R. B. Dell, H. N. Ginsberg, and W. V. Brown. 1986. Kinetic analysis using specific radioactivity data. *Methods Enzymol.* **129**: 384–395.
- Silver, D. L., N. Wang, and A. R. Tall. 2000. Defective HDL particle uptake in ob/ob hepatocytes causes decreased recycling, degradation, and selective lipid uptake. *J. Clin. Invest.* **105**: 151–159.
- Rigotti, A., E. R. Edelman, P. Seifert, S. N. Iqbal, R. B. DeMattos, R. E. Temel, M. Krieger, and D. L. Williams. 1996. Regulation by adrenocorticotrophic hormone of the in vivo expression of scavenger receptor class B type I (SR-BI), a high density lipoprotein receptor, in steroidogenic cells of the murine adrenal gland. *J. Biol. Chem.* **271**: 33545–33549.
- Rinninger, F., M. Brundert, S. Jäckle, P. R. Galle, C. Busch, J. R. Izbicke, X. Rogiers, D. Henne-Bruns, B. Kremer, C. E. Broelsch,

- et al. 1994. Selective uptake of high-density lipoprotein-associated cholesteryl esters by human hepatocytes in primary culture. *Hepatology*. **19**: 1100–1114.
26. Wiegand, C., C. Frenzel, J. Herkel, K. J. Kallen, E. Schmitt, and A. W. Lohse. 2005. Murine liver antigen presenting cells control suppressor activity of CD4⁺CD25⁺ regulatory T cells. *Hepatology*. **42**: 193–199.
27. He, T. C., S. Zhou, L. T. Da Costa, J. Yu, K. W. Kinzler, and B. Vogelstein. 1998. A simplified system for generating recombinant adenoviruses. *Proc. Natl. Acad. Sci. USA*. **95**: 2509–2514.
28. Giaccone, G., J. Battey, A. F. Gazdar, H. Oie, M. Draoui, and T. W. Moody. 1992. Neuromedin B is present in lung cancer cell lines. *Cancer Res.* **52**(9 Suppl.): 2732s–2736s.
29. Jokinen, E. V., K. T. Landschulz, K. L. Wyne, Y. K. Ho, P. K. Frykman, and H. H. Hobbs. 1994. Regulation of the very low density lipoprotein receptor by thyroid hormone in rat skeletal muscle. *J. Biol. Chem.* **269**: 26411–26418.
30. Moore, K. J., E. D. Rosen, M. L. Fitzgerald, F. Randow, L. P. Andersson, D. Altshuler, D. S. Milstone, R. M. Mortensen, B. M. Spiegelman, and M. W. Freeman. 2001. The role of PPAR-gamma in macrophage differentiation and cholesterol uptake. *Nat. Med.* **7**: 41–47.
31. Heeren, J., T. Grewal, S. Jäckle, and U. Beisiegel. 2001. Recycling of apolipoprotein E and lipoprotein lipase through endosomal compartments in vivo. *J. Biol. Chem.* **276**: 42333–42338.
32. Merkel, M., B. Loeffler, M. Kluger, N. Fabig, G. Geppert, L. A. Pennacchio, A. Laatsch, and J. Heeren. 2005. Apolipoprotein AV accelerates plasma hydrolysis of triglyceride-rich lipoproteins by interaction with proteoglycan-bound lipoprotein lipase. *J. Biol. Chem.* **280**: 21553–21560.
33. Nilsson-Ehle, P., and M. C. Schotz. 1976. A stable, radioactive substrate emulsion assay of lipoprotein lipase. *J. Lipid Res.* **17**: 536–541.
34. Lowry, O. H., N. J. Rosebrough, A. L. Farr, and R. J. Randall. 1951. Protein measurement with the folin phenol reagent. *J. Biol. Chem.* **193**: 265–275.
35. Yokode, M., R. E. Hammer, S. Ishibashi, M. S. Brown, and J. L. Goldstein. 1990. Diet-induced hypercholesterolemia in mice: prevention by overexpression of LDL receptors. *Science*. **250**: 1273–1275.
36. Skottova, N., R. Savonen, A. Lookene, M. Hultin, and G. Olivecrona. 1995. Lipoprotein lipase enhances removal of chylomicrons and chylomicron remnants by the perfused rat liver. *J. Lipid Res.* **36**: 1334–1344.
37. Goudriaan, J. R., M. A. M. den Boer, P. C. N. Rensen, M. Febbraio, F. Kuipers, J. A. Romijn, L. M. Havekes, and P. J. Voshol. 2005. CD36 deficiency in mice impairs lipoprotein lipase-mediated triglyceride clearance. *J. Lipid Res.* **46**: 2175–2181.
38. Pittman, R. C., T. P. Knecht, M. S. Rosenbaum, and C. A. Taylor. 1987. A nonendocytotic mechanism for the selective uptake of high density lipoprotein-associated cholesterol esters. *J. Biol. Chem.* **262**: 2443–2450.
39. Glass, C. K., R. C. Pittman, G. A. Keller, and D. Steinberg. 1983. Tissue sites of degradation of apoprotein A-I in the rat. *J. Biol. Chem.* **258**: 7161–7167.
40. McKay, I. R. 2003. Hepatoimmunology: from horizon to harborside. *In* Liver Immunology. M. E. Gershwin, J. M. Vierling, and M. P. Manns, editors. Hanley and Belfus, Philadelphia. 15–30.
41. Vassiliou, G., and R. McPherson. 2004. A novel efflux-recapture process underlies the mechanism of high-density lipoprotein cholesteryl ester-selective uptake mediated by the low-density lipoprotein receptor-related protein. *Arterioscler. Thromb. Vasc. Biol.* **24**: 1669–1675.
42. Rinninger, F., T. Kaiser, W. A. Mann, N. Meyer, H. Greten, and U. Beisiegel. 1998. Lipoprotein lipase mediates an increase in the selective uptake of high-density lipoprotein-associated cholesteryl esters by hepatic cells in culture. *J. Lipid Res.* **39**: 1335–1348.
43. Gwynne, J. T., and D. D. Mahaffee. 1989. Rat adrenal uptake and metabolism of high density lipoprotein cholesteryl ester. *J. Biol. Chem.* **264**: 8141–8150.
44. Love-Gregory, L., R. Sherva, L. Sun, J. Wasson, T. Schappe, A. Doria, D. C. Rao, S. C. Hunt, S. Klein, R. J. Neuman, et al. 2008. Variants in the CD36 gene associate with the metabolic syndrome and high-density lipoprotein cholesterol. *Hum. Mol. Genet.* **17**: 1695–1704.
45. Densuoonorn, N., Y. A. Carpentier, R. Racine, F. M. Murray, T. Seo, R. Ramakrishnan, and R. J. Deckelbaum. 2008. CD36 and proteoglycan-mediated pathways for (n-3) fatty acid-enriched triglyceride-rich particle blood clearance in mouse models in vivo and in peritoneal macrophages in vitro. *J. Nutr.* **138**: 257–261.
46. Nassir, F., B. Wilson, X. Han, R. W. Gross, and N. A. Abumrad. 2007. CD36 is important for fatty acid and cholesterol uptake by the proximal but not distal intestine. *J. Biol. Chem.* **282**: 19493–19501.